A Stochastic Model for Hyphal Growth

K. Sugden,[1] M. R. Evans,[1, 2] and W. C. K. Poon[1]

[1]SUPA, School of Physics, University of Edinburgh, Mayfield Road, Edinburgh EH9 3JZ

[2]Isaac Newton Institute for Mathematical Sciences, 20 Clarkson Road, Cambridge, CB3 0EH

(Dated: April 19, 2006)

We propose a simple model for filamentous fungal growth inspired by the role of microtubule-transported vesicles. We embody the dynamics of mass transport along a quasi-one-dimensional hypha with mutually excluding particles hopping on a growing one-dimensional lattice. We derive and analyse mean-field equations for the model and present a phase diagram of its steady state behaviour, which we compare to simulations. We discuss our results in the context of the observed growth properties of the filamentous fungus, *Neurospora crassa*.

Biologically, fungi [1] are intermediate between animals and plants. Apart from their intrinsic interest, fungi (especially yeasts) function as important animal models. They are also important sources of antibiotics (e.g. penicillin) and other biochemical products, and are responsible for a large fraction of annual world crop spoilage.

Filamentous fungi grow by the polarised extension of thread-like hyphae, which make up the body, or mycelium, of a fungus. Except for branching (which initiates new hyphae) the site of growth is localised to a single area at the tip of each elongating hypha. Enzymes and raw materials for growth are transported to the growth zone from other parts of the mycelium, allowing growth to continue through areas of poor nutrient content.

There are many theoretical models for the growth of fungal colonies and of single hyphae (reviewed in [2, 3]). Most models of single hypha growth concentrate on biomechanics [4, 5]. Of more interest for us here is the 'vesicle supply centre' (VSC) model [6, 7], in which raw materials for growth (packaged in vesicles) are distributed to the hyphal surface from a single 'supply centre' (sometimes identified with an organelle known as the spitzenkörper, or apical body) situated away from the growing tip. This class of models is capable of predicting the shape of hyphal tips; but the speed of growth (equivalent to the speed of the VSC) is an input parameter. Moreover, all transport processes are subsumed into a single rate of vesicle supply at the VSC. We are aware of just one model that takes explicit account of transport along the growing hypha [8]. A main interest of this early work, however, was the initiation of branching; moreover, these authors did not relate vesicle transport to growth velocity. This latter issue remains poorly understood.

In this letter, we propose a model which makes an explicit connection between the long-distance transport of nutrients along a hypha and its resulting extension as they reach the site of growth. Our model details the movement of nutrients towards the tip, and is controlled by the rate at which nutrients enter the system and the efficiency with which they extend the length of the hypha. We demonstrate that by altering these rates, steady states can be attained whereby the hypha is extending at a constant rate while being supplied with nutrients far behind the tip. Our model has features in common with [8]. Like [8], we use computer simulations, but unlike [8], we can also make analytical progress because of recent advances in non-equilibrium statistical physics.

Our model is inspired by the well-known Totally Asymmetric Simple Exclusion Process (TASEP). Originally introduced as a lattice model of ribosome motion along mRNA [9], recent variants have been widely used to model the collective dynamics of molecular motors [10–13]. The application of this and other classes of statistical mechanical models to many kinds of 'biological traffic' has recently been reviewed [14]. The TASEP is also widely studied in its own right as a fundamental model of non-equilibrium statistical mechanics [15], in particular as a simple driven diffusive system exhibiting non-equilibrium phase transitions [16] between different macroscopic density and current regimes [17, 18]. Our work contributes to the study of both 'biological traffic' and non-equilibrium phase transitions.

To model fungal growth, we introduce a new feature into the TASEP: particles reaching the end of the lattice will act to extend it. We ask whether a constant input rate far from the growing end can generate steady state lattice growth and if so, how the growth velocity depends upon the system parameters. We find that, as in the TASEP, different macroscopic regimes exist in this growing system, with different forms for the growth velocity, and non-equilibrium phase transitions between these regimes. Moreover, we find one steady state regime which holds similarities with the observed vesicle concentrations inside a growing fungal hypha.

To arrive at the model we recall that materials for growth are packaged in vesicles, and these are carried to the growth site by kinesin 'walking' on microtubule filaments running length-ways through the hypha. Once at the site of growth, they fuse with the hyphal wall, resulting in localised extension [1, 19, 20]. A kinesin motor with 'cargo' progressing toward the tip will encounter a number of microtubule segments, detaching from one and
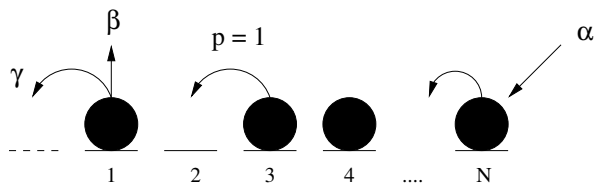
FIG. 1: Schematic of the hypha model with input rate α, hopping rate $p = 1$, absorption rate β and growth rate γ.

attaching to another on its way. The net result can be approximated to a continuous, directed motion of mass toward the hyphal tip. We thus devise our model by supposing that a hypha contains a number of *effective* microtubule tracks which run *continuously* to the tip.

Each effective microtubule is modelled by a 1-D lattice, and the kinesin motors plus cargo by particles which hop between lattice sites. We identify lattice site 1 as the hyphal tip. Particles obey hard-core exclusion and hop in one direction without overtaking, towards the tip. Particles arriving at the tip act to extend the lattice through the transformation: *particle → new site.*

We justify our model with a quick order of magnitude test. We identify the lattice repeat with the kinesin step size, 8 nm [21]. In the model organism *Neurospora crassa*, $\lesssim 10^3$ vesicles fuse with the tip per second and the tip growth velocity is $\sim 1 \, \mu m/s$ [22]. Thus, the extension by one lattice unit in the model ($\lesssim 10$ nm) is equivalent to the arrival of order 10 vesicles. If each particle delivered to the end contributes to lattice extension, we require ~ 10 equivalent effective microtubules in a typical hyphal cross section, an acceptable estimate.

The model dynamics are specified by the rates at which the following processes occur on the lattice: particles in the bulk hop toward the tip with rate 1; particles enter the lattice far from the tip with rate α; particles detach from site 1 with rate β and transform into a new lattice site with rate γ, as shown schematically in Fig. 1. Thus γ is the parameter controlling the lattice growth rate and β represents processes where particles reach the end but do not contribute directly to growth.

We perform Monte Carlo model simulations by stochastically updating particles on a lattice according to the above dynamics. After some relaxation time, density profiles are obtained by averaging site occupancies over many updates. We find three different macroscopic behaviours. Results for representative parameter values $\alpha = 0.25$, $\beta = 0$ and γ in the range 0.2 to 0.56, are shown in Fig. 2. For high values of γ one sees profiles that decay from the tip to a γ-independent bulk density equal to α. For the highest values of γ the density at the tip is $< \alpha$. As γ is lowered the tip density is $> \alpha$ and the region over which the decay occurs grows in size. For low values of γ we see distinct profiles where the bulk density is γ-dependent and is $> 1/2$. The transition from
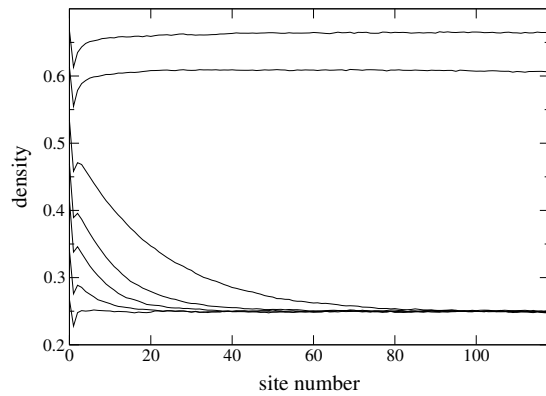

FIG. 2: Average site occupancy for $\alpha = 0.25$. Upper two traces are for $\gamma = 0.2$ (higher) and 0.24 (lower). Lower five traces (highest to lowest) for $\gamma = 0.28 - 0.56$ display apical peaks and decays.

the high γ to the low γ profiles is discontinuous and involves a jump in the bulk density. In the regime of high α and γ, density profiles with algebraic decays between the boundaries are observed. These are 'maximal current' profiles, which we shall discuss shortly.

We now seek an analytical understanding of our observations using a mean-field approximation where we consider the average density, $\rho_i(t)$ at site i, and ignore correlations between the density at different sites [17]. We describe the growth dynamics in a frame of reference co-moving with the growing tip. The tip site is always labelled site 1. Each time growth occurs, all other site labels must therefore be updated $i \rightarrow i + 1$. The change in density at site i is the net result of particles entering from the site on the right, departing to the site on the left and shifting right due to index relabelling during growth. Within the mean-field approximation, we have, for $i > 2$,

$$\frac{d\rho_i}{dt} = \rho_{i+1}[1 - \rho_i] - \rho_i[1 - \rho_{i-1}] + \gamma\rho_1[\rho_{i-1} - \rho_i] \, . \quad (1)$$

Note that the third term is proportional to the rate at which lattice sites are added, $\gamma\rho_1 = v$ which is the tip velocity. Separate equations govern the change in density at sites 1 and 2, in order to take into account the effect of the *particle → new site* transition:

$$\frac{d\rho_1}{dt} = \rho_2[1 - \rho_1] - (\gamma + \beta)\rho_1 \, , \quad (2)$$

$$\frac{d\rho_2}{dt} = \rho_3[1 - \rho_2] - \rho_2[1 - \rho_1] - \gamma\rho_1\rho_2 \, . \quad (3)$$

Eq. 3 differs from the bulk equation only in that should a growth event occur, there is never particle at site 2 after the lattice indices are updated. The final term is hence a decrease in density at site 2.

Finally, since particles enter at rate α, the particle density at the right-hand end is effectively α. As the lattice grows, this boundary recedes from the tip with velocity $-v$, ultimately corresponding to right boundary condition

$$\lim_{N \to \infty} \rho_N = \alpha \ . \tag{4}$$

We seek a steady state solution for this system defined in the reference frame of the tip. Such a solution is characterised by a constant current of particles everywhere through the system, a uniform tip velocity and a density profile which decays to the right boundary condition over a finite length scale, so that the profile is effectively independent of the system size, i.e. we seek solutions to (1–3) with the time derivatives set to zero and obeying the boundary condition (4). We obtain an expression for the particle current through the system in the tip's stationary frame from Eq. 1

$$J = \rho_i[1 - \rho_{i-1}] - v\rho_{i-1} \ . \tag{5}$$

Now, at the tip $J = (\gamma + \beta)\rho_1 = (1 + \beta/\gamma)v$, whereas far away from the tip (5) yields $J = \alpha(1 - \alpha - v)$, so that

$$v = \frac{\alpha(1 - \alpha)}{1 + \alpha + \beta/\gamma} \ , \tag{6}$$

which gives the tip velocity in terms of α and β/γ.

We now restrict ourselves to $\beta = 0$, and comment on the effects of non-zero β later. Since for $\beta = 0$ the tip velocity is simply a result of a flux of particles through the final lattice site, we have $J = v$ and thus from (5) a recurrence relation relating the steady state density at any site to that at the previous site:

$$\rho_i = \frac{v(1 + \rho_{i-1})}{1 - \rho_{i-1}} \quad i > 2 \ . \tag{7}$$

We define $\rho_\infty = \alpha$ as the stable fixed point value to which this recurrence relation converges:

$$\rho_\infty = \alpha = \frac{1 - v - \sqrt{1 - 6v + v^2}}{2} \ . \tag{8}$$

The decay length to α is finite and independent of lattice size, as required. We are now able to solve for all densities in terms of the parameters, α and γ:

$$\rho_1 = \frac{v}{\gamma} \ = \ \frac{\alpha[1 - \alpha]}{\gamma\alpha + \gamma} \ , \tag{9}$$

$$\rho_2 = \frac{v}{1 - \rho_1} \ = \ \frac{\gamma\alpha[1 - \alpha]}{\gamma[\alpha + 1] - \alpha[1 - \alpha]} \ , \tag{10}$$

and for $i > 2$, ρ_i is given through (7).

Under our constraint that the bulk density is α, we find two types of steady-state solution to the mean-field equations. In these solutions the profiles decay exponentially toward $\rho = \alpha$ and are distinguished by whether ρ
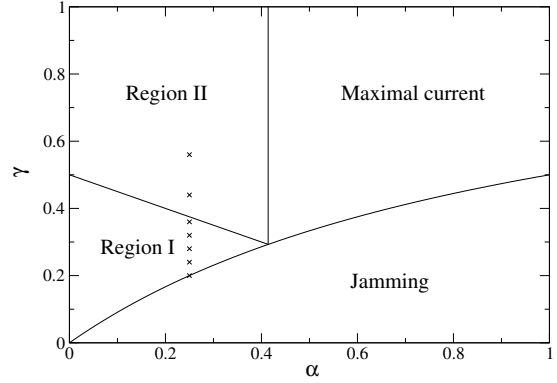

FIG. 3: Mean-field phase diagram for the model with $\beta = 0$. Phases are discussed in the text. Sample points for Monte Carlo simulations of Fig. 2 are marked with x's

decays to α from above or below. For $\gamma > (1 - \alpha)/2$, which we refer to as region I, the decay is from above and for $\gamma < (1 - \alpha)/2$, which we refer to as region II, the decay is from below, from a minimum value at site 2, although there is a peak in the density at site 1.

However these steady state solutions only exist in certain parameter regimes. For $\gamma < \alpha/(1 + \alpha)$, instead of iterating to the fixed point (8), the density is fixed for $i > 1$ at $\rho_i = 1 - 2\gamma$, with $\rho_1 = v/\gamma$ and $v = \gamma(1 - 2\gamma)/(1 - \gamma)$. The interpretation is that the rate of release of particles at the growing end is no longer large enough to control the input rate. Thus the particle density reaches a maximum value that extends from near the tip throughout the whole lattice and the boundary condition (4) is not satisfied. This is not a steady state solution for our model in the sense we have defined and we describe this region as a 'jammed' phase. At the transition to the jammed phase the bulk density jumps discontinuously from $\rho = \alpha = \gamma/(1 - \gamma)$ to $\rho = 1 - 2\gamma$.

We see from (8) that the maximum value of α is $\alpha_c = \sqrt{2} - 1$, which is obtained when $v = 3 - 2\sqrt{2}$. For $\alpha > \alpha_c$, Eq. 1 no longer has real fixed points, and again we do not satisfy the boundary condition (4). We may understand the region bounded by $\alpha > \sqrt{2} - 1$ and $\gamma > \alpha/(1 + \alpha)$ as a maximal current phase, where the particles have reached a maximum flow rate through the system which is no longer limited by the input and growth rates. In this case, the density profile decays algebraically from the boundary sites 1 and N to a bulk density $\rho = \sqrt{2} - 1$ and does not constitute a steady state in our sense since the densities evolve as the system grows.

We summarise the results of the mean-field theory in a phase diagram in Fig. 3. Regions I and II correspond to the Monte Carlo profiles observed for high γ (Fig. 2), and the jammed region corresponds to the profiles observed
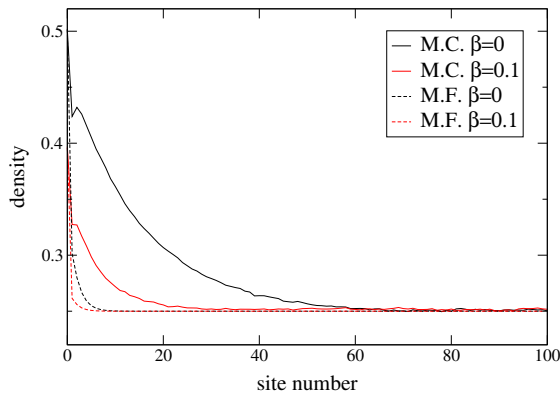
FIG. 4: Mean-field density profiles compared to MC density profiles for $\beta = 0$ and $\beta > 0$. $\alpha = 0.25$, $\gamma = 0.3$

for low γ. Simulations carried out over the whole parameter space revealed that the qualitative behaviour of the mean-field theory is correct, however, the transitions between different profile types do not occur exactly at the predicted mean-field boundaries. In order to compare in more detail the mean field and Monte Carlo results we plot in Fig. 4 mean-field and simulation profiles in region I. The decay length at the tip is significantly higher in the simulation, by a factor of about 10. These differences between mean-field theory and simulations can be attributed to density fluctuations and correlations in the system which are ignored in the mean-field theory.

We also plot in Fig. 4 the results of simulation and mean-field theory with a non-zero β. We find that the qualitative shape of the profile is not affected. A detailed analysis of the phase structure with $\beta \neq 0$ will be given elsewhere [24].

The steady state of region I, showing a uniform profile with a density peak at the tip is particularly interesting because in many species of filamentous fungus a region of increased vesicle concentration immediately behind the growing tip is observed [1]. The cause of this density gradient is not understood, however it is always present during growth, disappears when growth stops, and moves to the side when growth changes direction. The length scale of the high density region in *N. Crassa* is $\lesssim 1\mu m$ [1, 22]. For representative parameter values $\alpha = 0.25$ and $\gamma = 0.24$, our Monte Carlo simulations predict a high density region extending over ~ 30 lattice sites, or ~ 240 nm. It is encouraging that this very simple model can yield steady-state growth dynamics, with an estimate for the region of vesicle accumulation that is consistent with observations [23].

Note that, in contrast to the vesicle supply centre model [6, 7], a growth velocity arises naturally for our model. At least within mean-field theory, this velocity is determined in a simple way by two key parameters: the rate α at which material is 'fed' into the system far away from the tip and the ratio β/γ representing the efficiency with which the cargoes fuse with the tip. It would be of interest to test this prediction experimentally, for example by using vesicle supply and fusion mutants[20].

Finally we mention that the phase diagram Fig. 3 is related to that of the open boundary TASEP [18]; we explore this correspondence in a future publication [24].

[1] J. Deacon, *Fungal Biology*, second edition, Blackwell, 2005
[2] J. I. Prosser, pp. 319–333, in *The Growing Fungus*, Eds., N. A. R. Gow and G. M. Gadd, Chapman and Hall, 1995
[3] M. Bezzi and A. Ciliberto, *Comments On Theoretical Biology*, **8**,585, 2003
[4] A.L. Koch, *Advances in Microbial Physiology*, **29**, pp301–366, 1983
[5] A. Goriely and M. Tabor *J. Theor. Biol.*, **222**, 211, 2003
[6] S. Bartnicki-Garcia, F. Hergert and G. Gierz, *Protoplasma*, **153**, 46, 1989; G. Gierz and S. Bartnicki-Garcia *J. Theor. Biol.*, **208**, 151, 2001.
[7] S. H. Tindemans, N.Kern and B.M. Mulder *J. Theor. Biol.*, **238**, 937, 2006.
[8] J. I. Prosser and A. P. J. Trinci *J. Gen. Microbiol.*, **111**, 153, 1979.
[9] C. T. MacDonald, J. H. Gibbs and A. C. Pipkin, *Biopolymers*,**6**, 1, 1968
[10] R Lipowsky, S Klumpp and Th M. Nieuwenhuizen *Phys. Rev. Lett.* **87**, 108101, 2001; S Klumpp and R Lipowsky *J. Stat. Phys.* **113**, 233 2003
[11] A Parmeggiani, T. Franosch and E. Frey *Phys. Rev. Lett* **90**, 086601, 2003; *Phys. Rev. E* **70**, 046101, 2004; M. R. Evans, R. Juhàsz and L. Santen, *Phys. Rev. E* **68**, 026117 2003
[12] G. A. Klein, K. Kruse, G. Cuniberti and F. Jülicher *Phys. Rev. Lett.* **94**, 108102, 2005
[13] O. Campas **et al.** q-bio.SC/0512018, 2006
[14] D. Chowdhury, A. Schadschneider and K. Nishinari *Phys. Life Revs.* **2**, 318, 2005
[15] D. Mukamel, pp237–258 in *Soft and Fragile Matter: Nonequilibrium Dynamics, Metastability and Flow*, Eds M. E. Cates and M. R. Evans, IoP Bristol 2000
[16] J. Krug *Phys. Rev. Lett.* **67**, 1882, 1991
[17] B. Derrida, E. Domany and D. Mukamel *J. Stat. Phys*, **69** 667
[18] B. Derrida, M. R. Evans, V. Hakim and V. Pasquier *J. Phys. A*, **26**, 1493 1993; G. Schütz and E. Domany, *J. Stat. Phys.*, **72**, 277, 1993
[19] N. A. R. Gow, in *The Growing Fungus*, Eds. N. A. R. Gow and G. M Gadd, Chapman and Hall, 1995, p. 277.
[20] S. Seiler, M. Plamann and M. Schliwa *Curr. Biol.*, **9**, 779, 1999.
[21] D. Bray *Cell Movements*, 2nd edition, Garland, 2000.
[22] A. J. Collinge and A. P. J. Trinci *Arch. Microbiol.*, **99**, 353, 1974.
[23] We should treat this comparion with caution: a real hy-

pha tapers at the tip; this has to be taken into account when comparing observed vesicle concentrations with site occupancy in our strictly 1D model.

[24] K. Sugden and M. R. Evans *in preparation*